



Pharmaceutical Nanotechnology

One-step preparation of chitosan solid nanoparticles by electrospray deposition

Shaoling Zhang, Kohsaku Kawakami*

Biomaterials Center, National Institute for Materials Science, International Center for Materials Nanoarchitectonics, 1-1 Namiki, Tsukuba, Ibaraki 305-0044, Japan

ARTICLE INFO

Article history:

Received 20 May 2010

Received in revised form 2 July 2010

Accepted 7 July 2010

Available online 14 July 2010

Keywords:

Electrospray deposition

Chitosan

Nanoparticle

ABSTRACT

Solid micro- and nanoparticles were prepared from chitosan/acetic acid solution in one-step by the electrospray procedure. The effects of various solution properties and processing parameters on particle formation were investigated. Solution viscosity and conductivity were the most important factors affecting electrospray behavior, i.e., stable electrospray was achieved only when viscosity was high and/or conductivity was low. Smaller particles could be obtained by decreasing acetic acid concentration, chitosan concentration, and/or flow rate. Furthermore, addition of ethanol could effectively stabilize the electrospray by decreasing the solution conductivity and increasing the solution viscosity. By optimizing the solution and operation parameters, the average diameter of the chitosan particles was reduced down to 124 nm, suggesting that electrospray is promising in producing solid micro- and nanoparticles for oral and pulmonary drug delivery systems.

© 2010 Elsevier B.V. All rights reserved.

1. Introduction

Nanoparticles are usually defined as particles with a diameter smaller than 100 nm. However, the definition for biomedical use is usually more liberal (Maeda, 2001; Reis et al., 2006; Vauthier and Bouchemal, 2009), partially due to distinctive features of particles of a few hundred nanometers, including 'enhanced permeability and retention effect' for injectable formulations (Maeda, 2001; Torchilin, 2006). Nanosuspensions for oral drug delivery typically contain particles with a diameter of a few hundred nanometers, which enhances dissolution rate (Kesisoglou et al., 2007; Van Eerdenbrugh and Van den Mooter, 2008). Pulmonary drug delivery is a noninvasive method for systemic drug administration, for which particle size plays an important role (Patton and Byron, 2007; Sung et al., 2007). As for dry powder administration, particles larger than 5 μm are trapped in the upper portion of the respiratory system. The optimal particle size for achieving maximum deposition in the deep lung is thought to be a few micrometers (Yang et al., 2008; Xie and Castracane, 2009), and thus marketed inhalable formulations usually fall within this size range. However, both theoretical models and experimental case studies suggest that more effective deposition may be achieved with particles with a diameter smaller than 100 nm (Smith, 1994; Jaques and Kim, 2000; Daigle et al., 2003).

Nanoparticulate drug carriers are usually formulated as suspensions (Reis et al., 2006; Vauthier and Bouchemal, 2009). However, solid nanoparticles are preferred, especially for oral and pulmonary

use. Although simple drying could be used for obtaining solid particles, it is time- and energy-consuming, and the particles usually suffer from the re-dispersivity problem. Electrospray deposition (ESD) is a direct method for preparing solid particles, and it can be conducted under mild conditions (Rietveld et al., 2006; Bagheri-Tar et al., 2007; Jaworek, 2007; Jaworek and Sobczyk, 2008). The electrospray process relies on coulomb repulsion to break the bulk liquid into fine charged droplets, which can be described by an electrochemical model (Gañán-Calvo, 1997; Hartman et al., 2000). Droplets emitted from the top of the solution cone, which was formed on the spray nozzle, are dried before reaching the target to form solid particles. Although electrospray has frequently been utilized to prepare biomedical nanofibers, investigations on producing nanoparticles are relatively rare (Xie et al., 2006a,b).

Chitosan is a natural polymer that has been studied extensively as a drug carrier, because it offers many advantages including biocompatibility, biodegradability, and bioadhesivity (Mitra et al., 2001; Agnihotri et al., 2004). In addition, its positive charge may overcome cellular barriers to enhance drug absorption. Thus, chitosan is investigated as a carrier for gene therapy as well (Lee et al., 2009; Tong et al., 2009; Jayakumar et al., 2010). However, chitosan nanoparticles are usually prepared as suspensions. In this study, ESD is employed to prepare chitosan solid nanoparticles for their wide use as the drug delivery carriers.

2. Materials and methods

2.1. Materials

Chitosan (chitosan 5) and acetic acid were purchased from Wako Pure Chemical, Osaka, Japan. Degree of deacetylation of chitosan

* Corresponding author. Tel.: +81 29 860 4424; fax: +81 29 860 4714.
E-mail address: kawakami.kohsaku@nims.go.jp (K. Kawakami).

was 80 mol/mol%, and its molecular weight was ca. 120 kDa as determined by gel permeation chromatography (Shodex GPC-101, Showa Denko, Tokyo, Japan) using pullulan as a molecular weight standard. Hexanol and ethanol were obtained from Nacalai Tesque, Kyoto, Japan. All chemicals were used without further purification. Ultrapure water was prepared using a water purification system (Milli-Q Biocel A10, Millipore, Billerica, MA, USA).

2.2. Solution properties

Generally, chitosan was dissolved in aqueous acetic acid. For simplicity, the solution with a chitosan concentration of Y g/L and acetic acid concentration of X , v/v% was expressed as $AXCY$. When ethanol was added, the expression was $AXCYEZ$, where ethanol concentration was Z , v/v%.

Surface tension of the solvent was determined using a maximum bubble pressure tensiometer KSV BPA-800P (KSV Instruments, Helsinki, Finland) at a fixed bubble lifetime of 0.1 s, where the surface tension was confirmed to almost reach equilibrium. Solution conductivity was measured using a conductivity cell attached to an Orion benchtop multimeter (Thermo Fisher Scientific, Waltham, MA, USA). The kinematic viscosity of the solution was measured using an Ubbelohde viscometer (Kusano Science, Tokyo, Japan). The absolute viscosity was calculated by multiplying it by density, which was determined by weight of a 5 mL solution in a volumetric flask.

2.3. Electrospray deposition (ESD)

Chitosan solutions were supplied by a syringe pump for spraying from the grounded nozzle. Aluminum foil was placed perpendicular to the nozzle as a deposition target, to which a high negative voltage was applied, as shown schematically in Fig. 1. Solutions were dispersed into droplets by an electrical field generated between the nozzle and target. The solvent was evaporated before reaching the target, where the solid particles collected.

All preparations were carried out in an acrylic chamber at room temperature. The humidity was controlled to be lower than 20%RH by flowing nitrogen gas. Processing parameters were as follows unless stated otherwise: applied voltage, -25 kV; nozzle diameter, 0.65 mm; flow rate of the feed solution, $8.3 \mu\text{L}/\text{min}$; distance between the nozzle and target H , 7 cm.

2.4. Particle size and morphology

Particle morphology was investigated by scanning electron microscopy (SEM) (S4800, Hitachi, Tokyo, Japan). Samples were

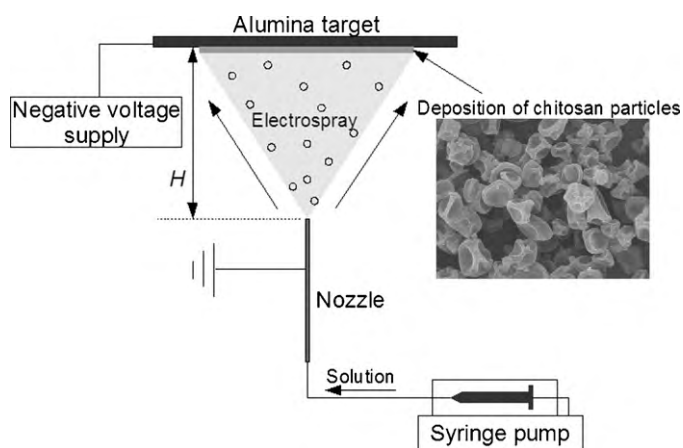


Fig. 1. Schematic diagram of the electrospraying apparatus. H is the distance between the nozzle and the target.

Table 1

Effect of chitosan concentration on the solution properties (acetic acid concentration 90, v/v%).

Chitosan concentration (g/L)	15	20	25	30	35	40
Conductivity ($\mu\text{S}/\text{cm}$)	200	290	338	374	448	488
Viscosity (mPa s)	32.4	41.0	80.7	113	198	346

sputter-coated using a platinum coater (E-1030 ion sputter, Hitachi, Tokyo, Japan) before measurements. Particle size was determined through the analysis of SEM pictures using Mac View ver. 4.0 software (Mountech, Tokyo, Japan). Three hundred particles were selected randomly from the image to obtain the Heywood diameter. Volume-mean diameter was used for the analysis.

3. Results and discussion

3.1. Effect of chitosan concentration

Table 1 shows the effect of chitosan concentration on the solution properties, when sufficient amount of acetic acid was contained (90, v/v%). With the increase in the chitosan concentration from 15 to 40 g/L, viscosity increased by more than an order of magnitude, from 32.4 to 346 mPa s. Although solution conductivity also increased with chitosan concentration, the increase was only 2.4-fold.

Fig. 2 shows typical SEM images and size distributions of particles obtained from chitosan solutions at concentrations of 20 and

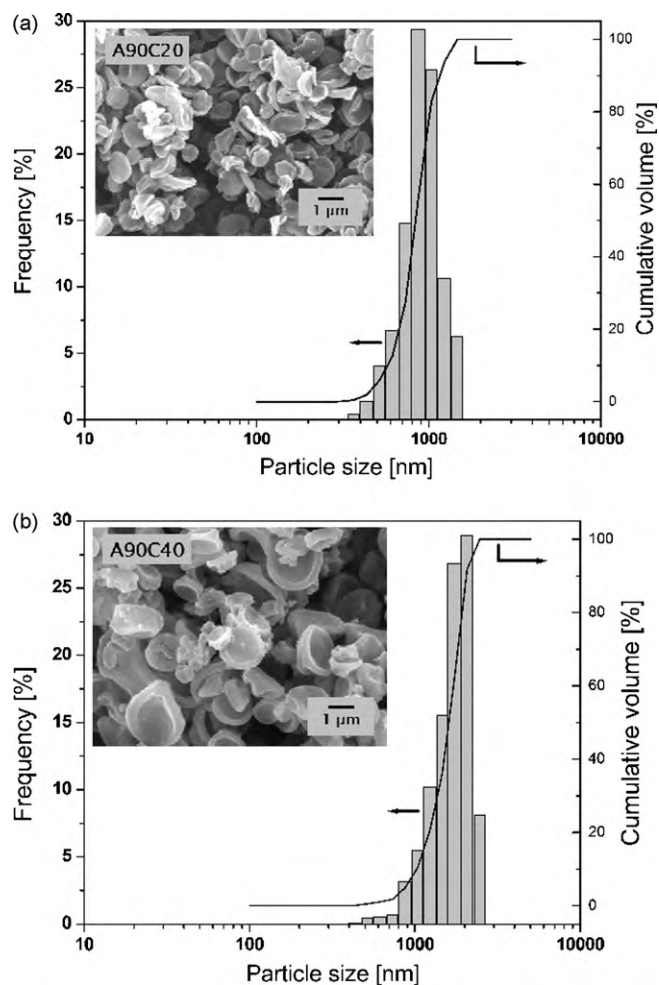


Fig. 2. SEM image and volume-mean size distribution of particles prepared from solutions (a) A90C20 and (b) A90C40.

40 g/L, that is, A90C20 and A90C40. The size distributions were monodisperse for both concentrations, as was the case for all preparations in this study. The size distribution shifted to higher values upon an increase in chitosan concentration. Cavities were found on the surface in both cases, which is a common shape for polymeric particles prepared by drying from droplets (Elvesson and Millqvist-Fureby, 2006; Vehring, 2008; Kawakami et al., 2010), and can be explained by the formation of a polymeric skin layer on the droplet surface at the early stage of drying, followed by shrinkage due to removal of the solvent.

The effect of chitosan concentration on average particle size is shown in Fig. 3. Particle size increased monotonically with chitosan concentration. Given that the droplet size was the same, particles obtained from droplets of higher concentration should be larger after solvent evaporation. Based on mass conservation, and assuming the final particles to be roughly spherical and homogeneous, particle diameter (d_p) and chitosan concentration (C) have the following relationship:

$$d_p = d \left(\frac{C}{\rho_p} \right)^{1/3} \quad (1)$$

where ρ_p is the density of the particles and d is droplet diameter. Thus, final particle size should be proportional to $C^{1/3}$. As shown in Fig. 3, the slope of particle size as a function of chitosan concentration was much steeper than 1/3, indicating factors other than concentration must be considered.

Increasing viscosity is thought to increase resistance of the solution to be separated into droplets (Hartman et al., 2000). A dimensionless number π_μ was introduced by Rosell-Llompart and Fernández la Mora (1994) to estimate the effect of viscosity on the droplet formation process:

$$\pi_\mu = \frac{(\gamma^2 \rho (\epsilon \epsilon_0 / K))^{1/3}}{\mu} \quad (2)$$

where ρ , γ , ϵ , μ and K are solution density, surface tension, dielectric constant, viscosity, and conductivity, respectively. For solutions having a value of $\pi_\mu \gg 1$, the effect of viscosity on droplet size is negligible. Otherwise, droplet size would increase with solution viscosity. Since the π_μ values for all solutions used in this study were smaller than 1, viscosity could be regarded as another factor for increasing particle size.

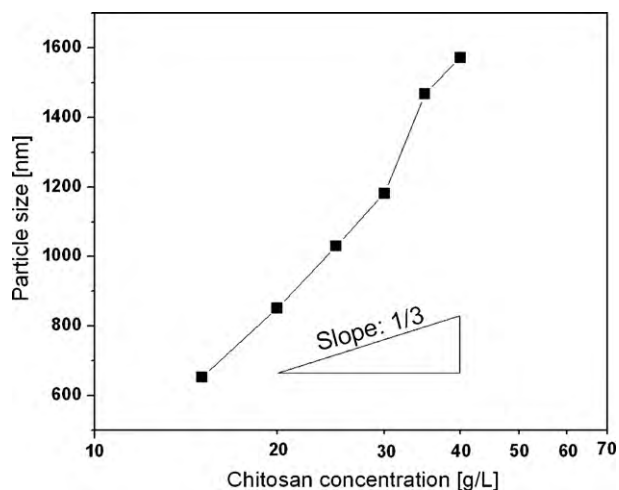


Fig. 3. Effect of chitosan concentration on particle size at an acetic acid concentration of 90, v/v%.

Table 2
Solution properties of A40C35 with different hexanol concentration.

Hexanol concentration (v/v%)	0	0.25	0.5	0.75	1.0	1.5
Conductivity (mS/cm)	2.84	2.81	2.81	2.77	2.74	2.67
Viscosity (mPa s)	125	139	142	142	144	145
Surface tension (mN/m)	43.2	39.6	38.4	35.8	34.9	32.2

3.2. Addition of hexanol (Effect of surface tension)

Electrospray is initiated when the coulomb repulsion in the solution is strong enough to overcome the surface tension. Therefore, surface tension could affect electrospray behavior. To study the effect of surface tension, hexanol was added to change the surface tension of the solution, without significantly changing other solution properties such as viscosity and conductivity. Surface tension could be varied relatively in a wide range at low acetic acid concentration. The properties of A40C35 solutions with various hexanol concentrations are listed in Table 2. The effect of hexanol concentration on particle size, and the representative SEM image of the chitosan particles are shown in Fig. 4.

Results showed almost no difference in particles with increasing hexanol concentration, indicating that the effect of surface tension on particle size and morphology is not significant under the experimental conditions employed in this study. Although the range of the surface tension values was limited in this study, this is a typical observation in the ESD technique. For example, Morota et al. (2004) revealed that a change in surface tension from 28 to 52 mN/m had no effect on the nanostructure of poly(ethylene oxide) films prepared by ESD. It should be noted that these discussions were based on equilibrium surface tension, which was not likely to be attained in the electrospray process. In the case of the spray-drying study, the surface tension at 10 ms exhibited good correlation with the droplet size produced from the spray nozzle rather than the equilibrium surface tension, and there was an indication that the surface tension in much shorter timescale might offer better correlation (Kawakami et al., 2010). Since the solutions used for the electrospray study are viscous compared to those for the spray-drying, there is a technical difficulty in determining the surface tension in the millisecond time scale. Such interfacial phenomenon in very short time scale seems to require further investigation.

3.3. Effect of acetic acid concentration

Properties of the chitosan solutions with various acetic acid concentrations are shown in Table 3. Conductivity sharply decreased

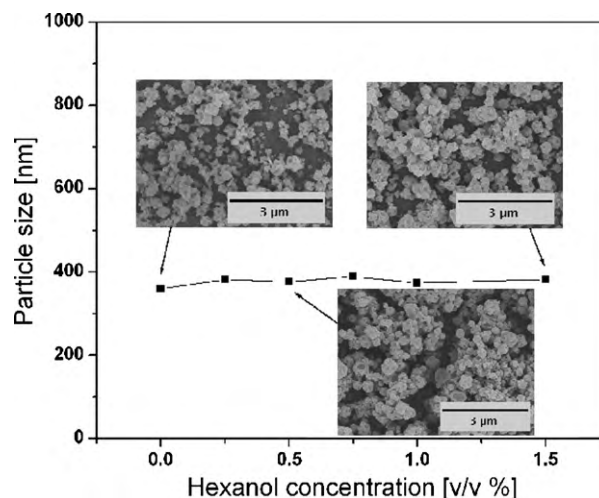


Fig. 4. Effect of hexanol concentration on particles prepared from solution A40C35.

Table 3
Effect of acetic acid concentration on the solution properties (chitosan 25 g/L).

Acetic acid concentration (v/v%)	50	60	70	80	90
Conductivity ($\mu\text{S}/\text{cm}$)	1826	1277	1001	564	338
Viscosity (mPa s)	71.2	73.5	85.5	93.9	80.7
Surface tension (mN/m)	39.8	38.4	35.7	34.2	32.2

upon an increase in acetic acid concentration from 50 to 90, v/v%, due to the low degree of dissociation of the acetic acid. No large difference was observed in solution viscosity, while surface tension decreased slightly upon an increase in acetic acid concentration (Geng et al., 2005).

Fig. 5 shows the relationship between acetic acid concentration and average particle size. Particle size increased with acetic acid concentration at all flow rates. Because conductivity was the only solution property dramatically influenced by acetic acid concentration, the increase in particle size can be explained by decreasing solution conductivity (Chen et al., 1995). The solutions could not be electro sprayed when acetic acid concentration was lower than 50, v/v% at a chitosan concentration of 25 g/L. This may be due to the relatively high conductivity and low viscosity, both of which decrease the stability of electro spray process (Jayasinghe and Edirisinghe, 2002).

Fig. 6 summarizes the effects of solution viscosity and conductivity on electro spray ability and particle size. Results show that electro spraying was not possible under conditions of high conductivity and/or low viscosity. An increase in conductivity increased the viscosity threshold (shown by a line in the figure) required for a successful electro spray. In addition, particle size could be reduced by increasing conductivity and decreasing viscosity. The smallest particle, which had a diameter of 360 nm, was obtained near the threshold line. As discussed in Section 3.1, higher viscosity enables stable operation and offers an increase in the droplet diameter. On the other hand, an increase in solution conductivity results in a decrease in the diameter due to enhanced coulomb repulsion. However, the electrical repulsion may be too strong to smoothly stretch out the surface of the solution into fine droplets above the viscosity/conductivity threshold line (Smith, 1986). Therefore, the electro spray process may become unstable at low viscosity/high conductivity conditions, preventing successful electro spray of the solution.

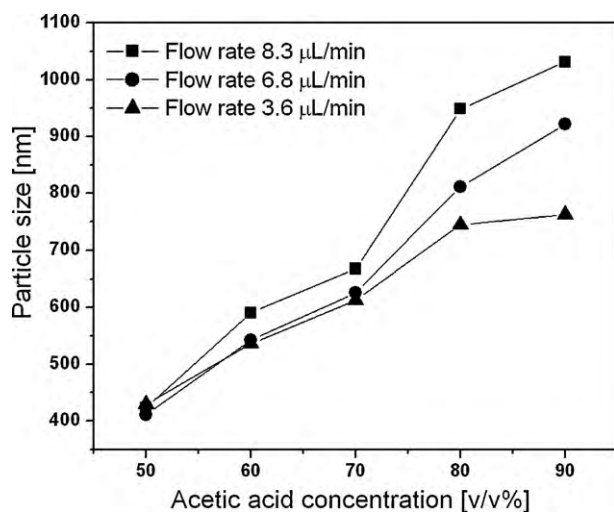


Fig. 5. Effect of acetic acid concentration on particle size at a chitosan concentration of 25 g/L.

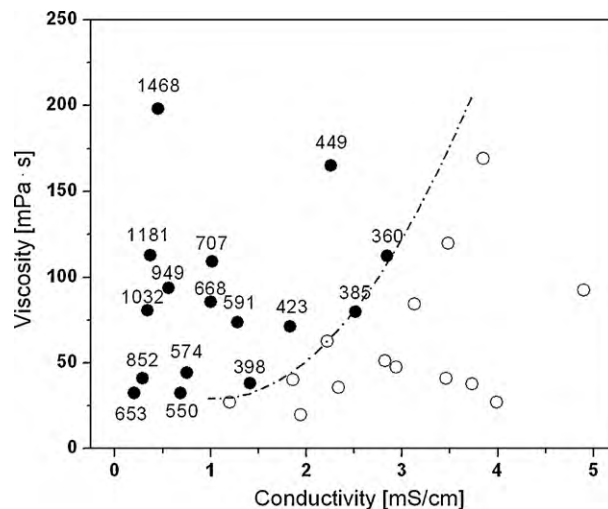


Fig. 6. Effect of solution viscosity and conductivity on electro spray ability and particle size. The line represents the threshold of electro spray ability. The open symbols exhibit solutions that could not be electro sprayed, and the numbers on the filled symbols indicate particle size (nm).

3.4. Addition of ethanol

The addition of ethanol to the aqueous media enables simultaneous changes in the solution conductivity, viscosity, and surface tension. The properties of solution A30C25 before and after addition of ethanol were summarized in Table 4. With the increase in ethanol concentration, conductivity and viscosity were decreased and increased, respectively. Thus, addition of ethanol should improve stability of the electro spray process based on the discussion in the previous section. As a matter of fact, the electro spray of A30C25 became possible only with the addition of ethanol. Fig. 7 shows effect of the ethanol concentration on the particle morphology. When the ethanol concentration was 10, v/v%, shape of the particles was not homogeneous. It became homogeneous with the increase in the ethanol concentration, which should be due to stabilization of the electro spray process.

Although many parameters including solution viscosity and conductivity were proved to affect the particle size significantly, threshold in the electro spray ability inhibited further decrease in the particle diameter as shown in Fig. 6. Therefore, addition of ethanol to the aqueous media should offer great improvement in the electro spray stability for achieving further reduction in the particle diameter as shown later.

3.5. Effect of operation parameters

Effect of the nozzle diameter was investigated from 0.50 to 1.20 mm, and the results showed that nozzle size was not an important parameter in our study (data not shown). The applied voltage and the distance from spray nozzle to the target have basically the same effect, because the strength of the electric field is determined by these parameters. For low conductive liquids, applied voltage has been regarded to have a significant effect on droplet size at large flow rates, at which droplet size decreased with increasing voltage (Tang and Gomez, 1996). In contrast, for highly conduc-

Table 4
Solution properties of A30C25 with different ethanol concentration.

Ethanol content (v/v%)	0	10	20	30	40	50
Conductivity ($\mu\text{S}/\text{cm}$)	2815	2073	1608	1223	914	630
Viscosity (mPa s)	51.0	71.9	88.3	100.0	108.3	164.9
Surface tension (mN/m)	46.5	39.0	35.4	33.0	30.6	28.8

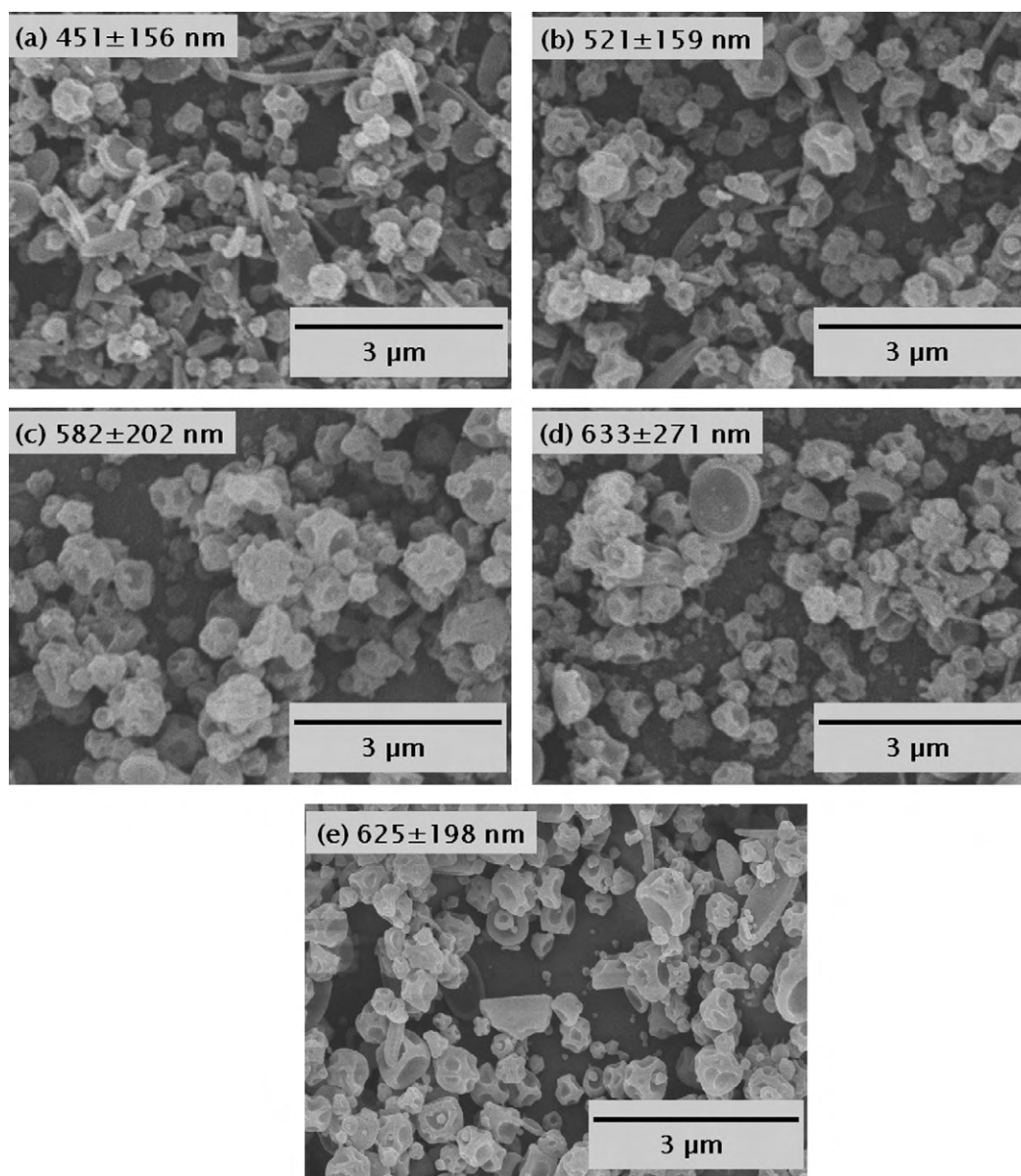


Fig. 7. SEM images of the chitosan particles prepared from A30C25 with the ethanol concentration: (a) 10, v/v%, (b) 20, v/v%, (c) 30, v/v%, (d) 40, v/v% and (e) 50, v/v%. Flow rate, 3.6 $\mu\text{L}/\text{min}$.

tive liquids, applied voltage has nearly no influence on droplet size (Rosell-Llompart and Fernández la Mora, 1994). In our case, particle size was insensitive to applied voltage, regardless of solution type and flow rate (data not shown). This was reasonable because the conductivities of the solutions used in this study were greater than 100 $\mu\text{S}/\text{cm}$, which could be regarded as highly conductive (Fernández de la Mora and Loscertales, 1994; Rosell-Llompart and Fernández la Mora, 1994).

Fig. 8 shows the effect of flow rate on particle size for the solutions A90C25, A70C25 and A50C25. When flow rate increased, particle size increased sharply for A90C25, while only slight increase was seen for A70C25 and the particle size of A50C25 remained nearly constant.

Droplet size d could be scaled by flow rate Q when highly conductive solutions were used (Fernández de la Mora and Loscertales, 1994; Rosell-Llompart and Fernández la Mora, 1994; Chen et al., 1995; Gañán-Calvo et al., 1997):

$$d \sim Q^{1/3} \quad (3)$$

According to Eq. (1), particle size is proportional to droplet size. Therefore, the same equation holds for the relation between particle size and flow rate. The slope values of the best fits for A90C25, A70C25 and A50C25 were 0.36, 0.16 and 0.04, respectively. The result for A90C25 was close to the value expected by the scaling law. However, as acetic acid concentration increased, the effect of flow rate on particle size became less significant. As shown in Table 3, solution conductivity drastically increased with decreasing acetic acid concentration. An increase in the charge carried by the electrospray reduces its stability because of strong electrostatic repulsions. Thus, the scaling law of Eq. (3) no longer applies in these situations (Jaworek and Krupa, 1999; Jaworek, 2007).

3.6. Reduction in the particle size

Based on the results obtained above, effective reduction in the particle size should be achieved at lower flow rate, lower chitosan concentration, and lower acetic acid concentration with the addition of ethanol. Fig. 9 shows the particles obtained at the optimized

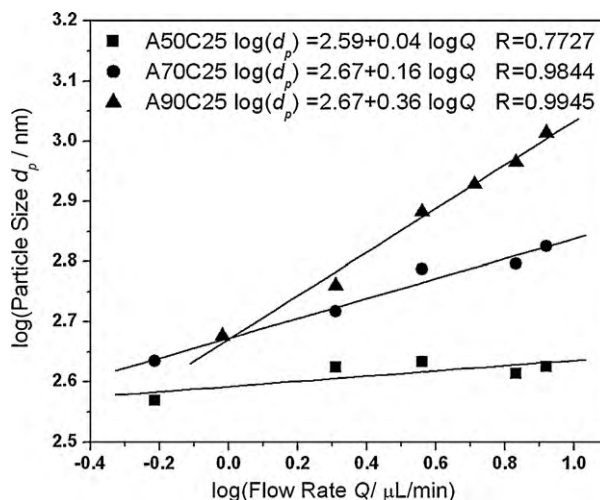


Fig. 8. Effect of flow rate on particle size.

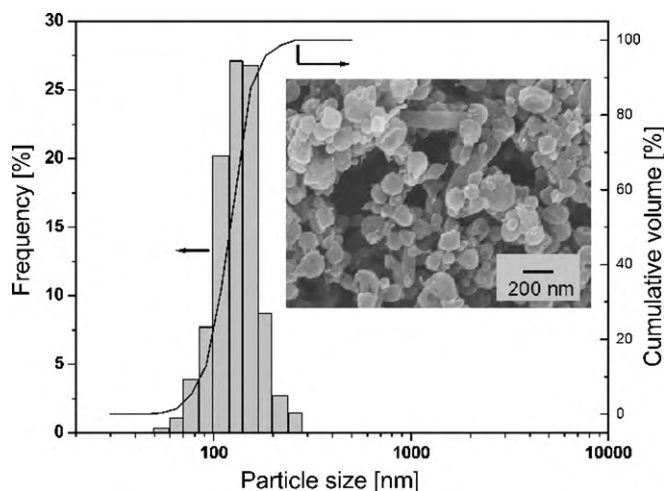


Fig. 9. The SEM image and volume-mean size distribution of the chitosan particles prepared from A30C10E20.

condition, where A30C10E20 was electrospayed at a flow rate of 0.6 $\mu\text{L}/\text{min}$. The particle size could be reduced to 124 nm. This size of particles have great advantages for both oral and pulmonary drug delivery in terms of increased dissolution rate and enhanced deposition in the deep lung, respectively. Although productivity was lowered by decreasing flow rate and concentration, it can be overcome to some extent with instrumental configuration including increase in the nozzle numbers.

4. Conclusions

One-step preparation method of chitosan solid micro- and nanoparticles using ESD technique was presented. Particle size could be controlled by altering the solution and operation parameters. The dominant solution characteristics were conductivity and viscosity. Particle size decreased upon an increase in conductivity or a decrease in viscosity. The most important operation parameter was the flow rate Q . Particle size increased with Q . Moreover, addition of ethanol to the aqueous media was effective to stabilize the electrospay behavior by changing the solution conductivity and viscosity. The smallest average particle size obtained in this series of experiments was 124 nm, which was prepared with the addition of ethanol. In addition to the simplicity of the preparation procedure, ESD has many advantages including its mild conditions

in the process. Thus, ESD should be a promising method for producing micro- and nanoparticulate solid formulations for oral and pulmonary drug delivery systems.

Acknowledgments

The authors thank Mr. Koji Funaba, Nanotechnology Innovation Center, National Institute for Materials Science, for helping gel permeation chromatography measurements. This work was in part supported by World Premier International Research Center (WPI) Initiative on Materials Nanoarchitectonics, MEXT, Japan.

References

- Agnihotri, S.A., Mallikarjuna, N.N., Aminabhavi, T.M., 2004. Recent advances on chitosan-based micro- and nanoparticles in drug delivery. *J. Control Release* 100, 5–28.
- Bagheri-Tar, F., Sahimi, M., Tsotsis, T.T., 2007. Preparation of polyetherimide nanoparticles by an electrospay technique. *Ind. Eng. Chem. Res.* 46, 3348–3357.
- Chen, D., Pui, D.Y.H., Kaufman, S.L., 1995. Electrospaying of conducting liquids for monodisperse aerosol generation in the 4 nm to 1.8 μm diameter range. *J. Aerosol Sci.* 26, 963–977.
- Daigle, C.C., Chalupa, D.C., Gibb, F.R., Morrow, P.E., 2003. Ultrafine particle deposition in humans during rest and exercise. *Inhal. Toxicol.* 15, 539–552.
- Elversson, J., Millqvist-Fureby, A., 2006. In situ coating—an approach for particle modification and encapsulation of proteins during spray-drying. *Int. J. Pharm.* 323, 52–63.
- Fernández de la Mora, J., Loscertales, I.G., 1994. The current emitted by highly conducting Taylor cones. *J. Fluid Mech.* 260, 155–184.
- Gañán-Calvo, A.M., 1997. Cone-jet analytical extension of Taylor's electrostatic solution and the asymptotic universal scaling laws in electrospaying. *Phys. Rev. Lett.* 79, 217–220.
- Gañán-Calvo, A.M., Dávila, J., Barrero, A., 1997. Current and droplet size in the electrospaying of liquids. Scaling laws. *J. Aerosol Sci.* 28, 249–275.
- Geng, X., Kwon, O., Jang, J., 2005. Electrospinning of chitosan dissolved in concentrated acetic acid solution. *Biomaterials* 26, 5427–5432.
- Hartman, R.P.A., Brunner, D.J., Camelot, D.M.A., Marijnissen, J.C.M., Scarlett, B., 2000. Jet break-up in electrohydrodynamic atomization in the cone-jet mode. *J. Aerosol Sci.* 31, 65–95.
- Jaques, P.A., Kim, C.S., 2000. Measurement of total lung deposition of inhaled ultrafine particles in healthy men and women. *Inhal. Toxicol.* 12, 715–731.
- Jaworek, A., 2007. Micro- and nanoparticle production by electrospaying. *Powder Technol.* 176, 18–35.
- Jaworek, A., Krupa, A., 1999. Classification of the modes of EHD spraying. *J. Aerosol Sci.* 30, 873–893.
- Jaworek, A., Sobczyk, A.T., 2008. Electrospaying route to nanotechnology: an overview. *J. Electrostat.* 66, 197–219.
- Jayakumar, R., Chennazhi, K.P., Muzzarelli, R.A.A., Tamura, H., Nair, S.V., Selvamurugan, N., 2010. Chitosan conjugated DNA nanoparticles in gene therapy. *Carbohydr. Polym.* 79, 1–8.
- Jayasinghe, S.N., Edirisinghe, M.J., 2002. Effect of viscosity on the size of relics produced by electrostatic atomization. *J. Aerosol Sci.* 33, 1379–1388.
- Kawakami, K., Sumitani, C., Yoshihashi, Y., Yonemochi, E., Terada, K., 2010. Investigation of the dynamic process during spray-drying to improve aerodynamic performance of inhalation particles. *Int. J. Pharm.* 390, 250–259.
- Kesisoglou, F., Panmai, S., Wu, Y., 2007. Nanosizing—oral formulation development and biopharmaceutical evaluation. *Adv. Drug Deliv. Rev.* 59, 631–644.
- Lee, D.W., Yun, K., Ban, H., Choe, W., Lee, S.K., Lee, K.Y., 2009. Preparation and characterization of chitosan/polyguluronate nanoparticles for siRNA delivery. *J. Control Release* 139, 146–152.
- Maeda, H., 2001. SMANCS and polymer-conjugated macromolecular drugs: advantages in cancer chemotherapy. *Adv. Drug Deliv. Rev.* 46, 169–185.
- Mitra, S., Gaur, U., Ghosh, P.C., Maitra, A.N., 2001. Tumour targeted delivery of encapsulated dextran-doxorubicin conjugate using chitosan nanoparticles as carrier. *J. Control Release* 74, 317–323.
- Morota, K., Matsumoto, H., Mizukoshi, T., Konosu, Y., Minagawa, M., Tanioka, A., Yamagata, Y., Inoue, K., 2004. Poly(ethylene oxide) thin films produced by electrospay deposition: morphology control and additive effects of alcohols on nanostructure. *J. Colloid Interface Sci.* 279, 484–492.
- Patton, J.S., Byron, P.R., 2007. Inhaling medicines: delivering drugs to the body through the lungs. *Nat. Rev. Drug Discov.* 6, 67–74.
- Reis, C.P., Neufeld, R.J., Ribeiro, A.J., Veiga, F., 2006. Nanoencapsulation I. Methods for preparation of drug-loaded polymeric nanoparticles. *Nanomed. Nanotechnol. Biol. Med.* 2, 8–21.
- Rietveld, I.B., Kobayashi, K., Yamada, H., Matsushige, K., 2006. Electrospay deposition, model, and experiment: toward general control of film morphology. *J. Phys. Chem. B* 110, 23351–23364.
- Rosell-Llompart, J., Fernández de la Mora, J., 1994. Generation of monodisperse droplets 0.3 to 4 μm in diameter from electrified cone-jets of highly conducting and viscous liquids. *J. Aerosol Sci.* 25, 1093–1119.

- Smith, D.P.H., 1986. The electrohydrodynamic atomization of liquids. *IEEE Trans. Ind. Appl.* IA-22, 527–535.
- Smith, H.Ed., 1994. ICRP Publication 66: Human Respiratory Tract Model for Radiological Protection. Pergamon, New York.
- Sung, J.C., Pulliam, B.L., Edwards, D.A., 2007. Nanoparticles for drug delivery to the lungs. *Trends Biotechnol.* 25, 563–570.
- Tang, K., Gomez, A., 1996. Monodisperse electrosprays of low electric conductivity liquids in the cone-jet mode. *J. Colloid Interface Sci.* 184, 500–511.
- Tong, H.J., Shi, Q., Fernandes, J.C., Liu, L., Dai, K.R., Zhang, X.L., 2009. Progress and prospects of chitosan and its derivatives as non-viral gene vectors in gene therapy. *Curr. Gene Ther.* 6, 495–502.
- Torchilin, V.P., 2006. Multifunctional nanocarriers. *Adv. Drug Deliv. Rev.* 58, 1532–1555.
- Van Eerdenbrugh, B., Van den Mooter, G., 2008. Top-down production of drug nanocrystals: nanosuspension stabilization, miniaturization and transformation into solid products. *Int. J. Pharm.* 364, 64–75.
- Vauthier, C., Bouchemal, K., 2009. Methods for the preparation and manufacture of polymeric nanoparticles. *Pharm. Res.* 26, 1025–1058.
- Vehring, R., 2008. Pharmaceutical particle engineering via spray drying. *Pharm. Res.* 25, 999–1022.
- Xie, J., Lim, L., Phua, Y., Hua, J., Wang, C.J., 2006a. Electrohydrodynamic atomization for biodegradable polymeric particle production. *J. Colloid Interface Sci.* 302, 103–112.
- Xie, J., Marijnissen, J.C.M., Wang, C., 2006b. Microparticles developed by electrohydrodynamic atomization for local delivery of anticancer drug to treat C6 glioma *in vitro*. *Biomaterials* 27, 3321–3332.
- Xie, Y., Castracane, J., 2009. High-voltage, electric field-driven micro/nanofabrication for polymeric drug delivery systems, electrostatic techniques and biomedical application. *IEEE Eng. Med. Biol. Mag.* 28, 23–30.
- Yang, W., Peters, J.I., Williams III, R.O., 2008. Inhaled nanoparticles—a current review. *Int. J. Pharm.* 356, 239–247.